Monitoring the energy variation of an electron linac using a Cerenkov detector

LI Shu-Wei(李树伟)[1,2;1)] WANG Yi(王义)[1,2] LI Jin(李金)[1,2] LI Yuan-Jing(李元景)[1,2]
KANG Ke-Jun(康克军)[1,2] LIN De-Xu(林德旭)[3] ZHANG Qing-Jun(张清军)[3]

[1] Department of Engineering Physics, Tsinghua University, Beijing 100084, China
[2] Key Laboratory of Particle & Radiation Imaging (Tsinghua University),
Ministry of Education, Beijing 100084, China
[3] Nuctech Company Limited, Beijing 100084, China

Abstract A new method to monitor the energy variation of a multi-energy electron linac by combining a Cerenkov detector and a CsI(Tl) detector is reported. The signals in the Cerenkov detector show an appreciable but different dependence on the energy of the electron linac from the traditional CsI(Tl) detector due to the particular response of the former to charged electrons with high velocity above threshold. The method is more convenient than the HVL (half-value layer) method which is commonly employed to calibrate the energy of an electron linac for real time monitoring. The preliminary validity of the method is verified in a dual-energy electron linac with 6 MeV and 3 MeV gears. Moreover, the method combining the Cerenkov detector and the CsI(Tl) detector is applicable to probe the X-ray spectrum hardened by the inspected material and may serve as a novel tool for material discrimination with effective atomic number in radiation imaging.

Key words electron linac, Cerenkov detector, Geant4

PACS 25.40.Cm, 28.75.Gz, 21.60.-n

1 Introduction

Material discrimination by the dual-energy method in high-energy X-ray imaging [1–5] requires monitoring the energy change and variation of the electron linac in real time. Now the most popular method to calibrate an electron linac is called the HVL (half-value layer) method, namely the half-value layer of the X-ray corresponds to a certain energy of the electrons from the linac [6,7]. But the HVL method is not practical to monitor the variation for adjusting the tested material thickness in real time. On the other hand, unlike kilovoltage X-ray beams from roentgen tubes, HVL of the megavoltage X-ray beams from electron linacs changes slowly with energy rariation [8]. However we do not intend to detail the comparison between the HVL method and the new method we report here.

Cerenkov detectors, widely used in high energy experiments, can be applied in monitoring the electron linac energy due to its particular response to high speed charged particles above the threshold. For an electron linac operating above several MeV, a change in the electron energy leads to a modification to the high energy tail of the bremsstrahlung spectra. Fig. 1 shows the calculated bremsstrahlung spectra of electrons bombarding on a thick target of tungsten with energies of 3, 4, 5 and 6 MeV using Geant4 packages. Careful inspection of the four spectra reveals that the maximum X-ray energy extends to the emitted electron energy while the peaks are similar at about 0.4 MeV. It is shown that a remarkable effect caused by switching the electron energy lies near the electron energy. More specifically, the relative contribution from the high energy X photons, namely above 1 MeV, increases with increasing electron energy. So a Cerenkov detector, being sensitive to the secondary high speed electrons produced by high energy X-ray via Compton scattering, shall be sensitive to energy variation in the electron linac. Then by combining the Cerenkov detector with a dose detector, being required for the incident X-ray photon's energy, we

---

Received 13 February 2009

1) E-mail: li-sw06@mails.tsinghua.edu.cn

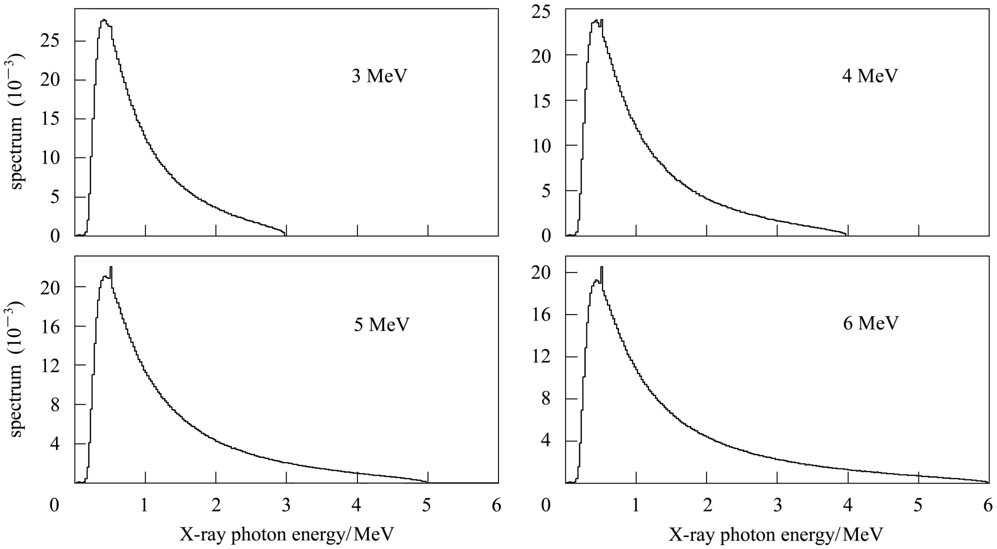

Fig. 1. The calculated bremsstrahlung spectra of different energy linacs.

could get information on the electron linac's energy variation. For convenience, we substitute a CsI(Tl) detector for the dose detector to fulfill the ideas in the following calculation and experiment.

2 The Cerenkov detector and experimental setup

If the secondary electrons produced in a translucent material are faster than light in the same medium [9, 10], Cerenkov light is emitted. The threshold condition is given by

$$\beta n > 1 \tag{1}$$

where β is the velocity of the fast electrons.

The yield of Cerenkov light with wavelengths from λ_1 to λ_2 is written as

$$N = 2\pi\alpha l\left(\frac{1}{\lambda_2}-\frac{1}{\lambda_1}\right)\left(1-\frac{1}{\beta^2 n^2}\right) \tag{2}$$

where N is the number of photons produced per electron, α is the fine structure constant. l is the path length of the electrons across the medium.

The Cerenkov detector used in our experiment and simulation is shown in Fig. 2(a). The Cerenkov emitter is made from quartz, which is one of the most frequently used materials to fabricate a Cerenkov detector because of its negligible fluorescence. The low limit of the wavelength is 200 nm and the density is 2.2 g/cm^3. The emitter is covered by a reflective layer of ESR made by 3M Company [11]. The outmost layer is a light-proof layer. Since the intensity of the X-ray beams on our device is sufficiently high and produces a rather high signal-to-noise ratio, we apply a photodiode instead of PMT as the readout unit, placed at one end of the Cerenkov emitter. In order to evaluate the nuclear counting effect, a second photodiode is glued at the upstream side of the former one but proofed with Cerenkov light. The length of the Cerenkov emitter along the incident direction of the X-ray is 250 mm. The width corresponding to the vertical distance from the photodiode to the X-ray beam axis is 50 mm and the thickness along the third dimension is 10 mm. A CsI(Tl) detector coupled with a photodiode as a readout unit is positioned immediately near the Cerenkov detectors. The size of the CsI(Tl) detector is 30 mm×10 mm×10 mm, that is, along the incident direction of the X-ray it is 30 mm and the sensitive area is 10 mm×10 mm.

The whole experimental setup is depicted in Fig. 2(b). The X-ray beam is confined in a very small angle by a collimator behind the production tungsten target. In front of the detector system, there is also a collimator to stop the scattering rays. Steel blocks with different thicknesses are placed before the second collimator for a further test of the applicability of the Cerenkov detector. The electron linac produced by Nuctech [5] has two nominal energy gears, 6 MeV and 3 MeV, denoted by AH and AL, respectively.

In the following experiment, for each energy gear, the accelerator operates in 10 Hz and the dose rate is 60 mGy/min at a spot 1 m away from the tungsten target. The width of the X-ray beam, at a detector spot 2 m away from the tungsten target, defined by the collimator is about 10 mm. For a detector sensitive area of 10 mm×10 mm, there are about 5.0×10^6 X-ray photons for 6 MeV and 7.0×10^6 for 3 MeV incident in a pulse, through calculation based on the spectrum shown in Fig. 1 and experimental setup.

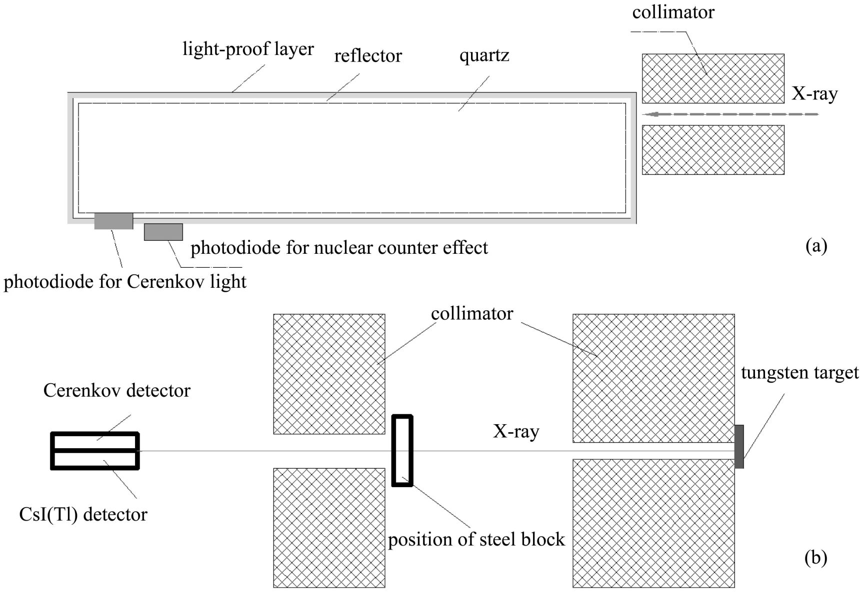

Fig. 2. The Cerenkov detector and experimental setup: (a) structure of the Cerenkov detector, (b) experimental setup.

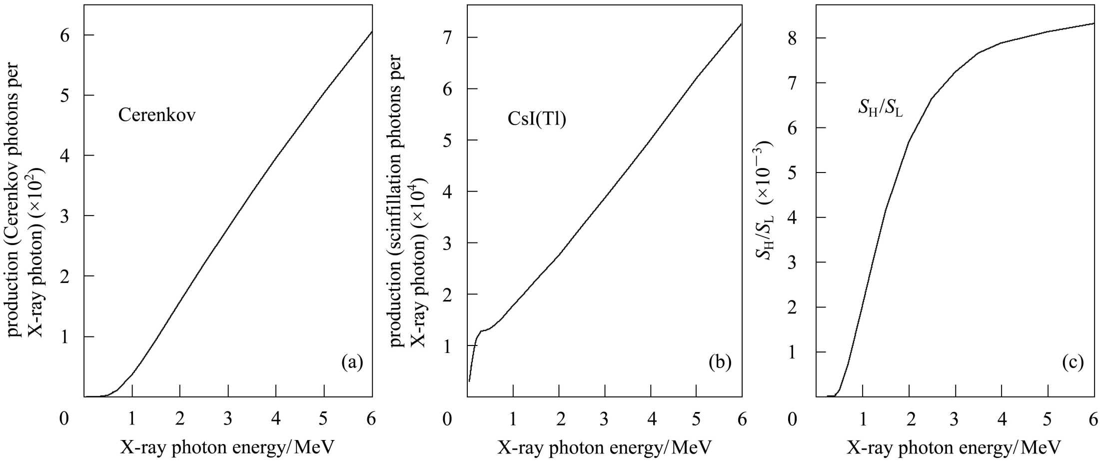

Fig. 3. Simulation result of an energy response comparison of the Cerenkov and CsI(Tl) detectors using the Geant4 package, and the response expressed by average production per monoenergetic X-ray photon incident on the detector sensitive area. (a) Energy response of the Cerenkov detector, expressed by average production of Cerenkov photons with wavelength limited from 200 nm to 1100 nm per X-ray incident on the sensitive area of the Cerenkov emitter. (b) Energy response of the CsI(Tl) detector, expressed by average production of scintillation photons per X-ray incident on the sensitive area of the CsI(Tl) detector. (c) Ratio of the two detectors' dependence on energy.

Although the output charge from the Cerenkov detector's photodiode is smaller than that from the CsI(Tl) detector's by an order of two or three, the sufficient intensity of the X-ray beam and the measurements based on the pulse mode ensure a dynamic range of above 4000 in the experiment. The preliminary validity of the method will be verified in 6 MeV and 3 MeV gears in the following.

3 Experimental and simulation results

The energy response calculated by Geant4 of the two types of detectors is plotted in Fig. 3. Both the Cerenkov and CsI(Tl) detectors' production increases with the energy of incident X-ray photons, but unlike the CsI(Tl) detector, no Cerenkov light is observed below 0.5 MeV. To inspect the effect of combining these two detectors, we further define a ratio of the signal in the Cerenkov detector (denoted by S_{H}) and the signal in the CsI(Tl) detector (denoted by S_{L}), $R=S_{\mathrm{H}}/S_{\mathrm{L}}$, and plot it as a function of X-ray energy in panel (c). It is found that the ratio increases with X-ray energy.

According to the energy response of the two detectors, for the Cerenkov detector, about 102 Cerenkov photons with wavelengths from 200 nm to 1100 nm are produced per incident X-ray photon on its sensitive area for the 6 MeV linac, and it drops to 44 Cerenkov photons for the 3 MeV linac; while for the CsI(Tl) detector, it change from 2.3×10^4 scintillation photons for the 6 MeV linac to 1.7×10^4 for the 3 MeV linac. So the Cerenkov detector is more sensitive to the linac's energy than the CsI(Tl) detector. The indicates the feasibility of monitoring the electron linac with a combination of these two detectors.

Figure 4 then presents the ratio as a function of the electron linac energy with Geant4 simulation. In order to avoid the uncertainty of calibration and compare with the experiment directly, the ratio is normalized to the value at 6 MeV as $M=R/R_0$. It is clearly seen that on decreasing the electron linac energy, the normalized ratio decreases significantly. Calculating the M value from the experimental data, it drops to 0.60 at 3 MeV, approaching the result of 0.56 from simulation.

In order to further prove the character difference between the Cerenkov detector and the traditional CsI(Tl) detector, the detectors were tested behind steel blocks with different thicknesses, as shown in Fig. 2(b). Fig. 5 presents the signals of the Cerenkov detector and the CsI detector at different thicknesses of the steel block. Similarly, the signals are normalized to the value with zero thickness in order to avoid calibration uncertainty and compare with the experiment directly. The four lines from up to down in both panels represent the energy of the electron linac of 6, 5, 4 and 3 MeV, respectively. The experimental results, available at 6 and 3 MeV, are presented by two symbols. First, the simulations are consistent with the experimental results. Second, it is found that the decreasing rate of the signal in the Cerenkov detector is smaller than that in the CsI(Tl) detector. This is due to the fact that the Cerenkov detector responds more to high energy X-rays that are less sensitive to the thickness of the blocking material.

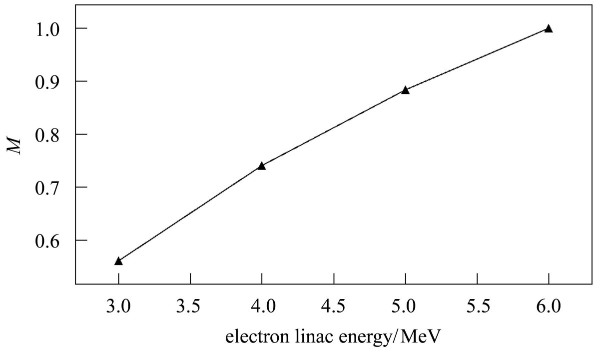

Fig. 4. The ratio as a function of the electron linac energy with Geant4 simulation.

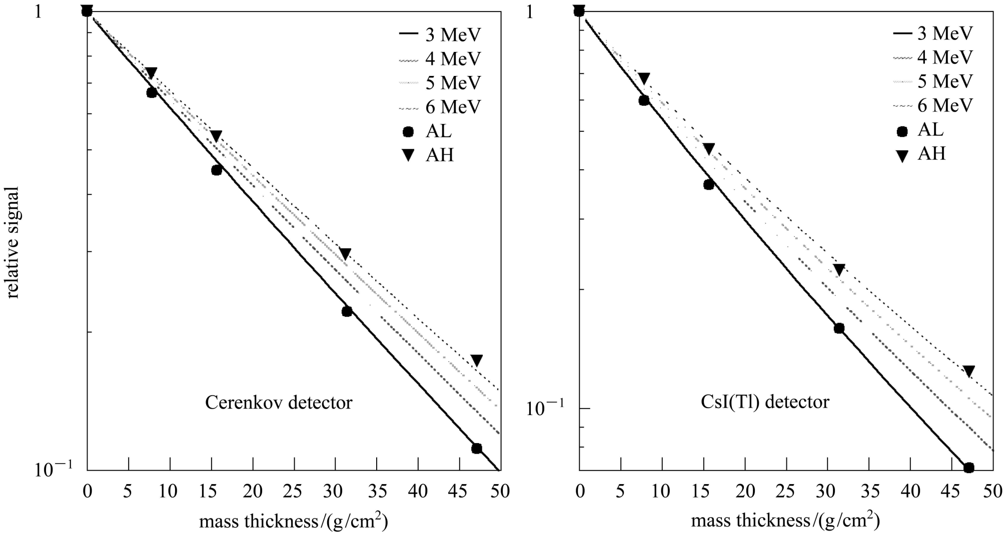

Fig. 5. Signals of the Cerenkov detector (left) and the CsI detector (right) at different thicknesses of the steel block. The lines are the results of Geant4 simulation, and the discrete symbols are the results of experiment.

4 Conclusions

In summary, a Cerenkov detector combined with a CsI(Tl) detector is applied to monitor the energy change of an electron linac in Nuctech for the first time. It is shown that due to the particular response of the Cerenkov detector to charged particles with high velocity, the signals in the Cerenkov detector exhibit sensitive responses to the change of electron linac energy. If optimizing the two types of detectors in material and geometry to increase the differences in energy response, a better result for monitoring the variations of electron linac should be achieved. Unlike the HVL method, the method used cannot tell the energy of the electron linac directly, but it is more convenient for real time measurement and may be more sensitive for monitoring the energy variation of the electron linac. Moreover, the method combining the Cerenkov detector and the CsI(Tl) detector is applicable to probe the X-ray spectrum hardened by the inspected material and may serve as a novel tool for material discrimination with effective atomic number in radiation imaging.

References

1 WANG Xue-Wu. PhD Dissertation. Tsinghua University, 2005 (in Chinese)

2 WU Xiao-Ping, CHEN Zhi-Qiang, WANG Xue-Wu et al. Nuelear Electronics & Detection Technology, 2005, **25**(6): 782 (in Chinese)

3 WANG Qi, CHEN Zhi-Qiang, WU Xiao-Ping et al. CT Theory and Applications, 2004, **13**(1): 32 (in Chinese)

4 WANG Xue-Wu, LI Jian-Min, KANG Ke-Jun et al. HEP & NP, 2007, **31**(11): 1076 (in Chinese)

5 http://www.nuctech.com

6 SHI Cheng-Yu, TANG Chuan-Xiang, LI Quan-Fen et al. Atomic Energy Science and Technology, 2001, **35**(6): 508 (in Chinese)

7 YAN Hui-Yong, TANG Chuan-Xiang, LI Quan-Feng et al. Atomic Energy Science and Technology, 2003, **37**(4): 372 (in Chinese)

8 Jerome A, Ravinder Nath. Medical Physics, 1985, **12**(1)

9 Jelley J V et al. Cerenkov Radiation and Its Applications. Pergamon Press, 1956

10 Knoll G F. Radiation Protection and Measurement. Third Edition. John Wiley & Sons, Inc.

11 http://www.3m.com